Two-Photon Ionization of 1,5-Anthraquinonedisulfonate via Photoinduced Electron Transfer

Martin Goez* and Valentin Zubarev

Fachbereich Chemie, Martin-Luther-Universität Halle-Wittenberg, Kurt-Mothes-Strasse 2, D-06120 Halle/Saale, Germany

Received: June 24, 1999; In Final Form: September 9, 1999

The photoreactions of the title compound with a variety of electron-transfer quenchers (e.g., methionine, triethylamine) in aqueous solution were investigated by laser flash photolysis with FT-EPR and optical detection. These systems proved to be efficient sources of hydrated electrons $e^{\bullet-}_{aq}$. The complex kinetics of the secondary reactions were modeled numerically, and the deceptively simple, seemingly first-order decay of $e^{\bullet-}_{aq}$ was analyzed. On the basis of the results of chemical control experiments and the dependence of the electron yield on the intensity of the exciting light, it was established that the pathway to $e^{\bullet-}_{aq}$ is a two-photon ionization, in which the first photon effects photoinduced electron transfer and the second photon ionizes the resulting radical anion. The novel feature of this mechanism compared to other two-photon ionizations with intervening chemical step is that it constitutes a catalytic cycle with respect to the substrate. Hence, the electron yield is not limited by substrate depletion and can significantly surpass the concentration of the starting material.

Photoinduced electron transfer (PET) leads to an activation of organic molecules in a similar way as electronic excitation does. However, the lifetimes of radical ions are often longer than those of electronically excited states because only bimolecular deactivation pathways are open to the former; the predominant one of these, charge recombination, can be slowed down by the use of polar solvents. Recently, we have shown that this kinetic advantage can be exploited to generate hydrated electrons $e^{\bullet-}_{aq}$ efficiently by a two-photon process consisting of a PET step followed by photoionization of the resulting radical anion.[1] The present paper probes mechanistic details and focuses on quantitative modeling of these photoreactions, especially as regards the secondary chemistry.

Most of our experiments were carried out by Fourier transform (FT) EPR spectroscopy, which lends itself extremely well to the study of PET reactions owing to its unique capability of identification and time-resolved monitoring of short-lived paramagnetic intermediates.[2] The only inherent drawback of this detection method, the inferior signal-to-noise ratio compared to UV/vis spectroscopy, is greatly alleviated by the electron spin polarizations (CIDEP),[3] which almost invariably accompany photoinduced radical reactions in magnetic fields.

Results and Discussion

Formation of $e_{aq}^{\bullet-}$ in PET Reactions of 1,5-Anthraquinonedisulfonate. This work was triggered by a totally unexpected observation[1a] (Figure 1, bottom) when we studied the system 1,5-anthraquinonedisulfonate/methionine (A/Met) in water by laser flash photolysis with FT-EPR detection as an extension of our previous photo-CIDNP investigations of PET-induced reactions of sulfur-containing amino acids.[4] We had chosen this sensitizer because it yields strong polarizations by the triplet mechanism.[5] At "normal" quinone concentrations (larger than about 2×10^{-3} M), we observed only the emission signal of the quinone radical anion $A^{\bullet-}$, which can be identified unambiguously by its EPR parameters.[5c] However, when we accidentally decreased the quinone concentration by a factor of 20, an additional emissive singlet with a *g* value of 2.000 55 appeared immediately after the laser flash and dominated the spectrum (compare the figure). The form and the extremely low *g* value of this signal suggest a hydrated electron $e^{\bullet-}_{aq}$, i.e., the occurrence of photoionization under these conditions. The efficiency of this process is remarkably high, as is already obvious from the trace shown: The ratio of the integrals of the singlet and the $A^{\bullet-}$ multiplet is approximately 4. Quantitative evaluation of the spectrum as described in the next section reveals that the absolute concentration of $e^{\bullet-}_{aq}$ is 1.6×10^{-4} M, about 60% *larger than that of the starting quinone*.

The all-emissive signals of $A^{\bullet-}$ evidence that the expected electron-transfer (ET) quenching of ^3A by the donor Met takes place and transfers the polarizations generated by the triplet mechanism to the radical ions. In contrast to the other systems discussed below, the donor radical cations $Met^{\bullet+}$ are not visible in the spectrum, although the triplet mechanism demands that their polarizations equal those of $A^{\bullet-}$. Their seeming absence is attributed to three factors that greatly reduce their peak heights. First, $Met^{\bullet+}$ is known to decay to other radicals with a half-life of about 220 ns;[6] the associated decay of the transverse magnetization during the acquisition time leads to line broadening by about 40 μT. Second, significantly larger intrinsic line widths are expected for this sulfur-containing radical cation compared to the narrow (3−5 μT) lines of $A^{\bullet-}$. Third, owing to its spin density distribution[4b] $Met^{\bullet+}$ exhibits 5 times more lines than does $A^{\bullet-}$. Because the combined effects must cause the peak heights of $Met^{\bullet+}$ to be lower than those of $A^{\bullet-}$ by at least 2 orders of magnitude, it is no wonder that the radical cations were not observed.

Coherence transfer from $Met^{\bullet+}$ to the subsequent radicals is negligible because the slow-exchange case is realized. Polarization transfer can occur but is not expected to lead to strong signals because $Met^{\bullet+}$ decays through several parallel reactions (combination with surplus substrate to give dimeric radical cations, decarboxylation to give α-amino alkyl radicals, and deprotonation to give α-thio alkyl radicals),[6] so the polarizations are spread out among several species and the individual lines become correspondingly weak; besides, relaxation losses in

* Author to whom correspondence should be addressed.

10.1021/jp992118b CCC: $18.00
Published on Web 11/04/1999

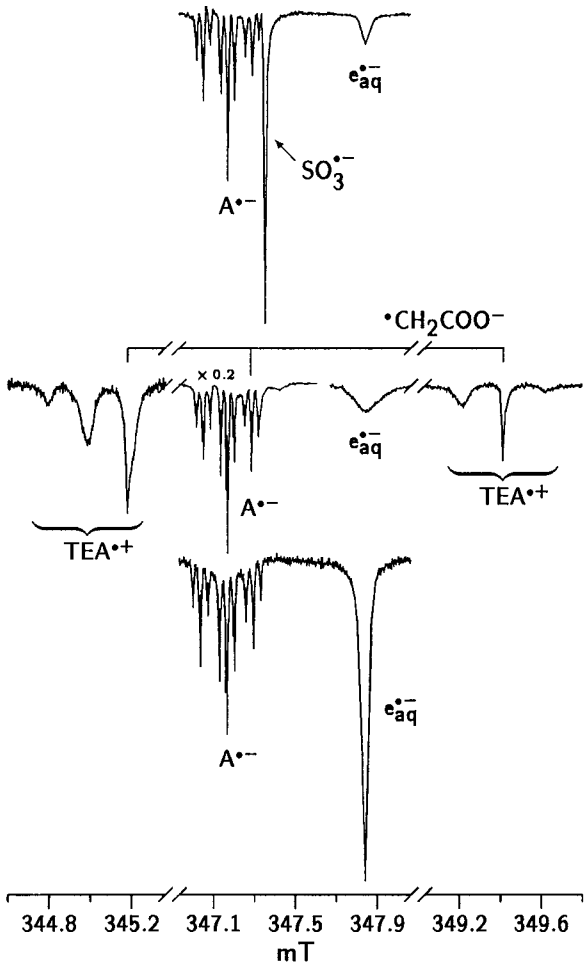

Figure 1. FT-EPR spectra during PET reactions of 1,5-anthraquinonedisulfonate A with different quenchers (bottom trace, 0.1 M methionine; center trace, 0.03 M triethylamine TEA with 5×10^{-3} M $ClCH_2COO^-$ added as an electron scavenger; top trace, 0.1 M SO_3^{2-}) in water. All traces show the resonances of the radical anion $A^{\bullet-}$ and the hydrated electron $e^{\bullet-}_{aq}$. Except for the methionine system, signals of the quencher-derived radicals (center trace, $TEA^{\bullet+}$; top trace, $SO_3^{\bullet-}$) are also present. The center trace further exhibits the triplet of $^{\bullet}CH_2COO^-$ formed by scavenging of $e^{\bullet-}_{aq}$. The intense $A^{\bullet-}$ multiplet in that spectrum totally obscures the center line of $^{\bullet}CH_2COO^-$ and the central signal group of $TEA^{\bullet+}$. To make the outer resonances more visible, this part of the spectrum has been reduced by a factor of 5. Other experimental parameters: operating frequency, 9.762 GHz; delay between laser flash and acquisition pulse, 30 ns; starting concentration of A, 1×10^{-4} M; pH between 10 and 11 (KOH).

$Met^{\bullet+}$ must be considered. At longer delays between the laser flash and the EPR acquisition pulse, we detected several very weak emissive lines, which we assign to the α-amino alkyl radical. The time dependence of the $A^{\bullet-}$ signal (see below) also provides indirect evidence for the intermediacy of this decay product of $Met^{\bullet+}$.

To confirm that the species with $g = 2.000\,55$ is indeed a hydrated electron, experiments with the electron scavengers N_2O and $ClCH_2COO^-$ were performed. It was ascertained that these scavengers react neither with the quinone triplet nor with its radical anion. With Met as the donor as well as in all other systems investigated, saturation of the solutions with N_2O completely suppressed the singlet. The $HO^{\bullet}$ radical produced by this reaction[7]

$$e^{\bullet-}_{aq} + N_2O \rightarrow N_2 + HO^- + HO^{\bullet} \qquad (1)$$

is unobservable owing to its short relaxation time[8] and because it is rapidly scavenged itself by Met,[6] ultimately giving unpolarized α-amino alkyl radicals. When $ClCH_2COO^-$ was employed at a concentration of 5×10^{-3} M (Figure 1, center), the singlet was found to be greatly decreased at 30 ns, the shortest possible delay between laser flash and EPR pulse, and the well-known triplet of the $^{\bullet}CH_2COO^-$ radical[9] appeared, also in emission:

$$e^{\bullet-}_{aq} + ClCH_2COO^- \rightarrow {}^{\bullet}CH_2COO^- + Cl^- \qquad (2)$$

The subsequent kinetic behavior (increase of the triplet at the same rate as decrease of the singlet) confirms that the species giving rise to the singlet is the precursor to $^{\bullet}CH_2COO^-$. These experiments and the magnetic parameters render beyond doubt the identification of the singlet as belonging to $e^{\bullet-}_{aq}$.

As the center trace of Figure 1 further shows, $e^{\bullet-}_{aq}$ is also formed with the donor triethylamine TEA. In the absence of $ClCH_2COO^-$, the yield of $e^{\bullet-}_{aq}$ is similar to that in the methionine case. With TEA, the (again emissive) signals of the radical cations $TEA^{\bullet+}$ can be clearly discerned in the spectra; their EPR parameters were identical with those reported in ref 5c. Integration reveals that immediately after the laser flash the polarizations of $TEA^{\bullet+}$ are comparable with the sum of polarizations of $A^{\bullet-}$ and $e^{\bullet-}_{aq}$.

Other quenchers were also tested. The top trace of Figure 1 displays the spectrum with SO_3^{2-} as the donor. The three emissively polarized species $A^{\bullet-}$, $e^{\bullet-}_{aq}$, and $SO_3^{\bullet-}$ can be clearly identified, the quenching reaction being

$$^3A + SO_3^{2-} \rightarrow A^{\bullet-} + SO_3^{\bullet-} \qquad (3)$$

The electron yield is lower in this system. We are inclined to attribute this mainly to an increased scavenging of $e^{\bullet-}_{aq}$ by impurities, which are either present in SO_3^{2-} from the start or formed during preparation of the rather concentrated solutions (0.1 M) and during the time needed to perform the measurements. This was corroborated by experiments with $ClCH_2COO^-$ added, which gave a sum polarization of $e^{\bullet-}_{aq}$ and $^{\bullet}CH_2COO^-$ that was higher than the polarization of $e^{\bullet-}_{aq}$ without this scavenger. This behavior is realized to an extreme with the quencher $S_2O_5^{2-}$, where only traces of $e^{\bullet-}_{aq}$ are observed besides the radicals $A^{\bullet-}$ and $SO_3^{\bullet-}$, which are expected for ET quenching:

$$^3A + S_2O_5^{2-} \rightarrow A^{\bullet-} + SO_3^{\bullet-} + SO_2 \qquad (4)$$

We ascribe the apparent low efficiency of electron formation to fast scavenging by surplus quencher according to

$$e^{\bullet-}_{aq} + S_2O_5^{2-} \rightarrow SO_3^{\bullet-} + SO_2^{2-} \qquad (5)$$

Again, the occurrence of significant $^{\bullet}CH_2COO^-$ polarizations when $ClCH_2COO^-$ is added to this system provides evidence for the initial formation of $e^{\bullet-}_{aq}$. The scavenging process of eq 5 was also sustained by laser flash photolysis experiments with optical detection, which showed that $e^{\bullet-}_{aq}$ produced by monophotonic ionization of the phenolate anion is rapidly scavenged by $S_5O_5^{2-}$. Lastly, quenching of ^3A by the amino acid alanine also led to formation of $e^{\bullet-}_{aq}$.

The fact that $e^{\bullet-}_{aq}$ is produced with this variety of quenchers clearly suggests that the species being photoionized is quinone-derived. To exclude the obvious process

$$^3A \xrightarrow{h\nu} A^{\bullet+} + e^{\bullet-}_{aq} \qquad (6)$$

SCHEME 1

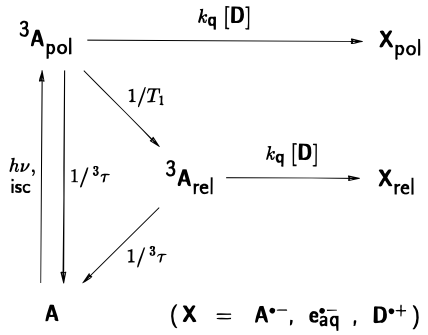

we carried out control experiments on A under the same conditions but without any quencher. Only insignificant amounts of $e^{\bullet-}_{aq}$ were detected in these measurements. Likewise, the donors were tested in the absence of the quinone and gave negative results only. This can only mean that the electron stems from the radical anion of the quinone, i.e., that in our experiments $A^{\bullet-}$ is photoionized according to

$$A^{\bullet-} \xrightarrow{h\nu} A + e^{\bullet-}_{aq} \tag{7}$$

Futher evidence for this is obtained from the dependence of the electron yield on the laser intensity (see pertaining section).

Quantitative Modeling of Secondary Kinetics. Kinetic measurements show a decrease of $e^{\bullet-}_{aq}$ with time, which is accompanied by an increase of $A^{\bullet-}$ (compare next section, Figure 3). The rates of these processes are seen to be connected and to depend on the starting concentration of A. The most natural explanation is by a reaction of $e^{\bullet-}_{aq}$ with surplus ground-state quinone according to

$$e^{\bullet-}_{aq} + A \xrightarrow{k_1} A^{\bullet-} \tag{8}$$

i.e., the reverse of process 7. However, owing to the high light intensities and, consequently, the high concentrations of reactive intermediates, second-order steps (e.g., charge recombinations) are also expected to play an important role in our experiments; this is borne out by the fact that the decay of the electron peak possesses a much larger amplitude than does the rise of the $A^{\bullet-}$ signal. For evaluation, the absolute concentrations of $e^{\bullet-}_{aq}$ and $A^{\bullet-}$ must thus be extracted from the measurements. This task involves relating the electron spin polarizations to the concentrations as well as determining the instrument sensitivity and the size of the illuminated volume; furthermore, it is necessary to take into account the instrumental response to fast kinetics.

Because only net polarizations by the triplet mechanism arise in these systems,[1a] a simple yet rigorous approach for quantitative modeling is to regard each chemical species X as occurring in a relaxed form X_{rel} and a polarized form X_{pol}, the former bearing the Boltzmann magnetization and the latter an opposite magnetization that is larger by a constant polarization factor $-P_0$. Sublevel-selective intersystem crossing of photoexcited ^1A produces ^3A spin-polarized by this factor ($P_0 = 200$).[5c] The relaxation time T_1 of the triplet is 5.5 ns;[5c] laser flash photolysis with optical detection gave rate constants k_q of 7.0×10^8 M^{-1} s^{-1} and 1.3×10^9 M^{-1} s^{-1} for quenching of ^3A by Met and TEA, respectively, and an unquenched chemical lifetime $^3\tau$ of 104 ns under our experimental conditions. Within the short duration of the laser flash, both electron spin relaxation of $e^{\bullet-}_{aq}$ and $A^{\bullet-}$ and the dark reactions of these intermediates can be neglected. The pertaining reaction scheme is displayed in Scheme 1.

With the integrated triplet generation rate being $[^3A]_0$, the total amount of initially present polarized radical anions is thus given by

$$[A^{\bullet-}_{pol}]_0 + [e^{\bullet-}_{aq,pol}]_0 = \frac{k_q[D]}{k_q[D] + 1/T_1 + 1/^3\tau}[^3A]_0 = \kappa[^3A]_0 \tag{9}$$

and that of relaxed radical anions by

$$[A^{\bullet-}_{rel}]_0 + [e^{\bullet-}_{aq,rel}]_0 = \frac{1/T_1}{k_q[D] + 1/T_1 + 1/^3\tau}\frac{k_q[D]}{k_q[D] + 1/^3\tau}[^3A]_0 = \frac{\kappa}{k_q[D]T_1 + T_1/^3\tau}[^3A]_0 = \frac{\kappa}{\lambda}[^3A]_0 \tag{10}$$

The initial ratio of polarized to relaxed species must be the same for $A^{\bullet-}$ and $e^{\bullet-}_{aq}$ because photoionization of the radical anion cannot depend on its electron spin state

$$\frac{[A^{\bullet-}_{pol}]_0}{[A^{\bullet-}_{rel}]_0} = \frac{[e^{\bullet-}_{aq,pol}]_0}{[e^{\bullet-}_{aq,rel}]_0} = \lambda \tag{11}$$

At the donor concentrations used ([Met] = 0.1 M, [TEA] = 0.03 M), we estimate λ to be 0.44 and 0.27, respectively, on the basis of the above data.

The apparent concentration $[X_{eff}]$ of species X is found by weighting the concentrations of its relaxed and polarized forms

$$[X_{eff}] = -P_0[X_{pol}] + [X_{rel}] \tag{12}$$

The sensitivity factor f of the spectrometer, which relates the concentration to the integrated signal intensity I, was obtained by measuring Fremy's salt under the same acquisition conditions as in our photoreactions. Only the illuminated fraction $1/g$ of the active volume contributes to the signal in a photo-CIDEP experiment, so one has

$$I = (f/g)[X_{eff}] \tag{13}$$

Because of the nonrectangular sample geometry and the fact that a focused laser beam had to be used, a determination of g from geometrical considerations was not feasible; estimates of g lie between 5 and 20. However, an accurate value of g can be extracted from the experimental data in a very simple way: Experimentally (see also below, Figure 6), the total concentration of $A^{\bullet-}$ immediately after the flash is found to become independent of the intensity of the exciting light when the latter is sufficiently high. Laser flash photolysis with optical detection showed that in the methionine and triethylamine systems the resulting limits of $[A^{\bullet-}]_0$ are 45.3% and 43.1% of the starting quinone concentration, respectively; moreover, the deviations of $[A^{\bullet-}]_0$ from these saturation values are smaller than 10% as long as the ratio $[e^{\bullet-}_{aq}]_0/[A^{\bullet-}]_0$ lies above 0.6. This condition was fulfilled in all experiments discussed here (for most of them, this ratio was about 3, corresponding to a deviation of less than 1%), so g was calculated from the signal of the radical anion, after deconvolution and extrapolation back to $t = 0$. The uncertainty introduced by this extrapolation—which was neces-

sary anyhow to obtain initial parameters for the numerical solution of the kinetic equations—is estimated to be marginal because the change of concentrations on that time scale is quite small (compare the figures below).

The duration of the $\pi/2$ acquisition pulse is not negligibly short on the time scale of the chemical kinetics. Therefore, deconvolution of the experimental intensities had to be performed (see Experimental Section).

With the initial intensity I_0 of the integrated $A^{\bullet-}$ signal (from the EPR experiments, after deconvolution) and the initial total concentration $[A^{\bullet-}]_0$ (from laser flash photolysis), eqs 11−13 yield

$$\frac{I_0}{f[A^{\bullet-}]_0} = \frac{1 - \lambda P_0}{g(1 + \lambda)} \tag{14}$$

Because P_0 and λ are known, g can thus be obtained from the data. However, we stress that this separation, which would be impossible on the basis of our EPR data alone, even in combination with the laser flash photolysis results, is completely unnecessary as long as the product λP_0 is significantly larger than unity, i.e., as long as the spin-polarized contribution to the signal dominates over the Boltzmann contribution; under these circumstances, the resulting term $-f\lambda P_0/[g(1 + \lambda)]$ simply constitutes a global sensitivity factor. As the values of P_0 and λ show, the condition $P_0\lambda \gg 1$ is certainly fulfilled in our systems. It is evident that the identical sensitivity factor must hold for the electron peak (as well as for any other species in this system that bears polarizations from the same source). Therefore, the initial concentrations of both $A^{\bullet-}$ and $e^{\bullet-}_{aq}$ are calibrated against an precisely known standard, namely, the saturation value of $[A^{\bullet-}]_0$.

For evaluation of the kinetic curves of the next section, λ was preset to the value resulting from eq 11, and g was then calculated from eq 14, using a fit of the $A^{\bullet-}$ integrals by a model function with iterative reconvolution according to eq 26 to obtain I_0; for this model function, the very simple form $a - b\exp(-ct)$ was found to be sufficient, as it approximated the experimental integrals with negligible deviations in all cases. While P_0 and g were kept fixed during the ensuing fit procedure, λ was allowed to vary within a small interval of ±50% to eliminate the extrapolation error by the exponential fit because the bimolecular steps in the reaction scheme exert their largest influence at early times.

The parameter λ derived above (eq 10) from Stern−Volmer considerations is expected to overestimate the actual value owing to the high light intensity in our experiments, which could well result in a significant participation of triplet−triplet annihilation or spin exchange; furthermore, the value of T_1 is not expected to be very accurate. However, repeating the evaluations with a different P_0 or λ (both up to a factor of 10 smaller) but at constant $(1 - \lambda P_0)/[g(1 + \lambda)]$ gave rate constants that did not change by more than about ±30%. Thus, the actual magnitudes of P_0, λ, and g exert only a weak influence on the results for the kinetic parameters.

A consistency test is also provided by the experiments with the electron scavenger $ClCH_2COO^-$. The $^{\bullet}CH_2COO^-$ signal is well-suited for this purpose because it obeys very simple kinetics, without complications by side reactions. A typical time dependence is displayed in Figure 2. The initial rise of the signal is due to reaction 2, the subsequent decay to electron spin relaxation of $^{\bullet}CH_2COO^-$, The constant of proportionality $\lambda P_0/(1 + \lambda)$ initially contained in the relationship between concentration and polarization reduces to unity in the course of the reaction. In contrast, g remains constant because on the time scale of the polarization kinetics diffusion is negligible. By comparing the maximum of the curve with the final value, the geometrical factor is thus eliminated, as are the precursor concentration and all Stern−Volmer factors deriving from reaction 8 and other decay processes of spin-polarized $e^{\bullet-}_{aq}$. A fit of the experimental curve to a biexponential function with constant floor after convolution according to eq 26 gave a value of 80 for $P_0\lambda/(1 + \lambda)$, which is 30% lower than that expected on the basis of the reported[5c] data, in accordance with the above reasoning.

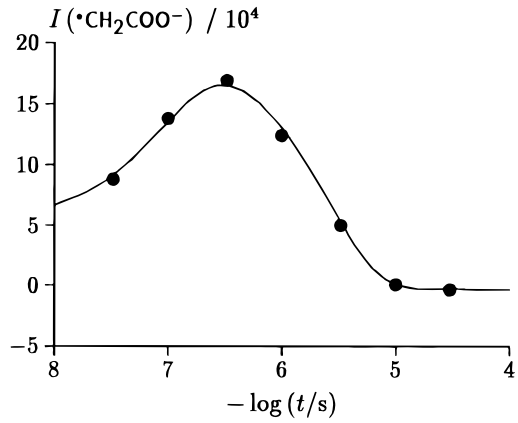

Figure 2. Time-dependent FT-EPR signal intensities (integrals) I of $^{\bullet}CH_2COO^-$ in the photoreaction of 1.15×10^{-4} M 1,5-anthraquinonedisulfonate in 0.1 M aqueous solution of KOH with 0.1 M methionine and 5×10^{-3} M electron scavenger $ClCH_2COO^-$. The solid line is a fit to a superposition of two exponentials and a constant term after iterative reconvolution according to eq 26.

Kinetic Scheme and Fit Results. Simulations were performed for the intensities (integrals) of $e^{\bullet-}_{aq}$ and $A^{\bullet-}$ in the Met and to some extent also the TEA systems; however, in the latter case a lower accuracy is expected owing to imperfect separation of the superimposed signals of $TEA^{\bullet+}$ and $A^{\bullet-}$. The systems of differential equations representing the kinetics were solved numerically.

The quinone triplet was not considered, and the reactions were described as starting at the radical stage. Initially present are thus A, $e^{\bullet-}_{aq}$, $A^{\bullet-}$, and the radical cation of the donor $D^{\bullet+}$. The concentration of the donor itself can be regarded as constant because it is much higher than that of the other species. Decarboxylation of $Met^{\bullet+}$ and deprotonation of $TEA^{\bullet+}$ yield α-amino alkyl radicals $D^{\bullet}$ as secondary radicals

$$D^{\bullet+} \begin{cases} \xrightarrow{k_{dec}} D^{\bullet} + CO_2 & D = \text{Met} \\ \xrightarrow{k_{dep}} D^{\bullet} & D = \text{TEA} \end{cases} \tag{15}$$

The former rate constant is known ($k_{dec} = 3.15 \times 10^6\ s^{-1}$);[6] the latter ($k_{dep}$ between 3×10^5 and $3 \times 10^6\ s^{-1}$, depending on pH) was determined separately by laser flash photolysis. The decarboxylation product CO_2 was also included in the kinetic scheme because it scavenges $e^{\bullet-}_{aq}$ with a rate constant of $7.7 \times 10^9\ s^{-1}$.[7]

The initial concentrations of the secondary species CO_2 and $D^{\bullet}$ were assumed to be zero; that of $A^{\bullet-}$ was obtained from the starting concentration of the quinone as explained above. An initial guess of $[e^{\bullet-}_{aq}]_0$ was taken from the EPR data after deconvolution and extrapolation back to $t = 0$ using the model function $p\exp(-qt)$, which was found to approximate the electron signal extremely well; $[e^{\bullet-}_{aq}]_0$ was then allowed to vary between 0.7 and 5 times this value to eliminate the extrapolation

error caused by the participation of bimolecular termination reactions of $e^{\bullet -}_{aq}$. The initial concentrations of $D^{\bullet +}$ and of A followed from the mass balance.

Besides the differential equations for the diamagnetic species (A; in the case of methionine also CO_2), four sets of differential equations, each comprising one equation for X_{rel} and one for X_{pol}, were used for the radical intermediates X ($e^{\bullet -}_{aq}$, $A^{\bullet -}$, $D^{\bullet +}$, and $D^{\bullet}$). Electron spin relaxation occurs within each set and effects unidirectional transitions from the polarized to the relaxed form. The chemical transformations are identical for the two forms and couple different sets without interconnecting relaxed and polarized species except for combinations of two radicals, which destroy polarizations by producing diamagnetic species from relaxed and polarized radicals alike. The initial concentrations of X_{rel} and X_{pol} followed from the chemical concentrations with eq 11. The uncertainty of λ, which would cause deviations of the balance between relaxed and polarized forms, is not crucial because it is accompanied by a compensating error in the geometrical factor, as discussed in the preceding section.

The spin−lattice relaxation times of $e^{\bullet -}_{aq}$ ($T_1 = 8\ \mu s$),[10] $A^{\bullet -}$ ($T_1 = 11\ \mu s$),[5c] and $D^{\bullet}$ ($T_1 = 1\ \mu s$)[11] have been reported. These parameters must depend on the experimental conditions to some degree, mainly on the radical concentrations owing to Heisenberg exchange; also some participation of electron scavenging by the donor, which is present in quite high concentration, cannot be excluded. To allow for this, the former two relaxation times were allowed to vary between 0.5 and 2 times the values given, the latter between 0.5 and 4 μs. Because the chemical transformations of $D^{\bullet +}$ according to eq 15 are fast compared to spin−lattice relaxation, T_1 of the radical cations was fixed at the literature value for $TEA^{\bullet +}$ (1 μs).[12]

Owing to the high concentrations, electron self-termination

$$e_{aq}^{\bullet -} + e_{aq}^{\bullet -} \xrightarrow{k_{self}} H_2 + 2HO^- \qquad (16)$$

must be taken into account. The rate constant k_{self} is 6×10^9 $M^{-1}\ s^{-1}$.[7]

Besides k_1 (eq 8), the rate constants to be varied included those of the charge recombinations

$$e_{aq}^{\bullet -} + D^{\bullet +} \xrightarrow{k_{2a}} D \qquad (17)$$

$$A^{\bullet -} + D^{\bullet +} \xrightarrow{k_{2b}} A + D \qquad (18)$$

and of secondary reduction of the substrate by the α-amino alkyl radical

$$A + D^{\bullet} \xrightarrow{k_3} A^{\bullet -} + \text{iminium cation} \qquad (19)$$

The intervals for the variations of these parameters (5×10^9 $M^{-1}\ s^{-1} < k_{1,3} < 2 \times 10^{10}$ $M^{-1}\ s^{-1}$, 5×10^9 $M^{-1}\ s^{-1} < k_{2a} < 4 \times 10^{10}$ $M^{-1}\ s^{-1}$, and 1×10^9 $M^{-1}\ s^{-1} < k_{2b} < 2 \times 10^{10}$ $M^{-1}\ s^{-1}$) were chosen because they are chemically reasonable.

The fit procedure is described in the Experimental Section. Figure 3 displays two examples of such fits, showing that both the short-time and the long-time behavior are reproduced correctly. Given the simple shape of the curves, it is not surprising that very good agreement between experimental and calculated intensities can be reached by using seven adjustable kinetic parameters. For the following reasons, we nevertheless believe that the obtained rate constants are meaningful. First, they are in line with expectations based on chemical intuition; despite the fact that we had chosen rather narrow constraining

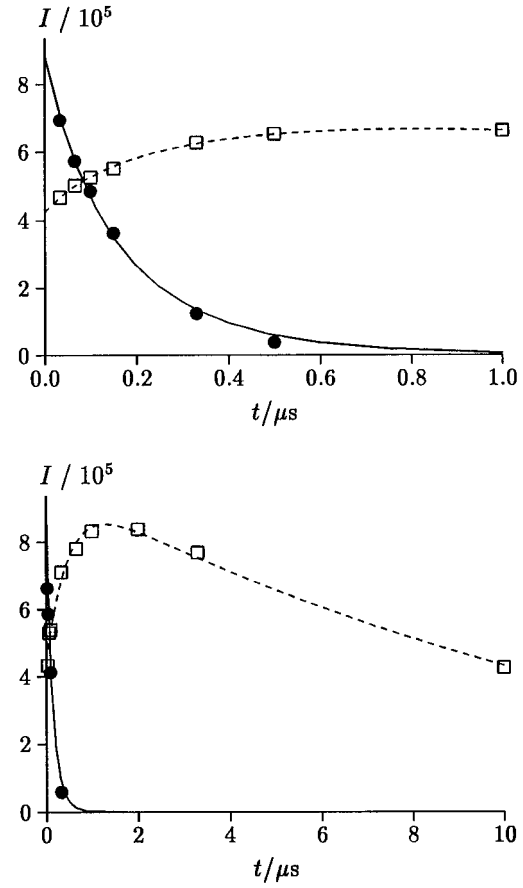

Figure 3. Best fits of the kinetic model described in the text to the experimental time dependence of the signal integrals *I*. Open squares and broken line, $A^{\bullet -}$; filled circles and solid line, $e^{\bullet -}_{aq}$. Quencher, 0.1 M Met; 0.1 M aqueous solution of KOH. The quinone concentrations were 3.3×10^{-4} (top) and 2×10^{-4} M (bottom).

TABLE 1: Kinetic Parameters Obtained from the Fits

parameter	k_1	k_{2a}	k_{2b}	$T_1(e^{\bullet -}_{aq})$	k_3	$T_1(A^{\bullet -})$	$T_1(D^{\bullet -})$
reaction	8	17	18		19		
best-fit value	16[a,c]	9.5[a,c]	1.7[a,c]	6[b,c]	8.5[a,d]	11[b,d]	3[b,d]

[a] In 10^9 $M^{-1}\ s^{-1}$. [b] In μs. [c] Error ±20%. [d] Error ±30%.

intervals, we furthermore did not observe any tendency of convergence at a border. Second, the best-fit rate constants are not all interdependent but fall into two separate sets, k_1, $k_{2a,b}$, and $T_1(e^{\bullet -}_{aq})$ influencing the early parts of both curves, k_3 and the other T_1 values influencing the long-time behavior of the $A^{\bullet -}$ signal only. Third, global optimizations of both curves at the same time were performed, which allows separation of the parameters contained in the first set. Last, similar rate constants were extracted from the fits throughout the concentration range of A studied (about 1 order of magnitude) and also with the two quenchers Met and TEA, which is to expected because k_1, $T_1(e^{\bullet -}_{aq})$, and $T_1(A^{\bullet -})$ are quencher-independent, the diffusion coefficients of $Met^{\bullet +}$ and $TEA^{\bullet +}$, which influence k_{2a} and k_{2b}, cannot differ significantly, and the α-amino alkyl radicals (k_3 and T_1 of $D^{\bullet}$) are almost identical.

Table 1 lists the kinetic parameters obtained in this way. A notable feature is that both k_{2a} and k_{2b} are smaller than k_1, i.e., that the charge recombinations according to eqs 17 and 18 are intrinsically slower processes than is scavenging of $e^{\bullet -}_{aq}$ by surplus starting quinone, eq 8. This might in part be due to the high ionic strength (about 0.1 M) of our samples, which decreases the rate constants of reactions between species of unlike charge and increases those between species of like charge

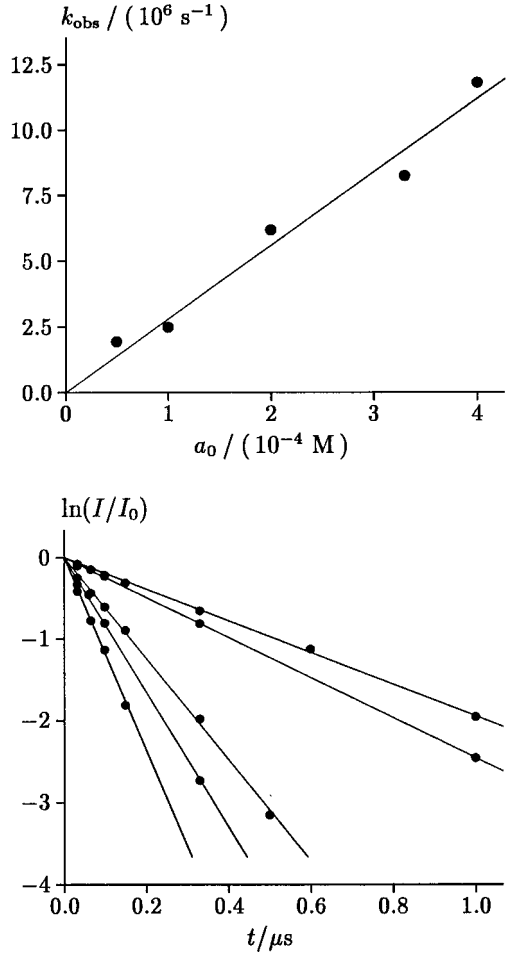

Figure 4. Bottom: time dependence of the relative signals (integrals) I/I_0 of the hydrated electron for different starting concentrations a_0 of 1,5-anthraquinonedisulfonate. Quencher, 0.1 M Met; 0.1 M aqueous solution of KOH; comparable light intensities in all experiments. Top: dependence of the slope k_{obs} of these plots on a_0. Slope of the regression line, 2.8×10^{10} M^{-1} s^{-1}.

(the quinonedisulfonate is deprotonated under our experimental conditions). However, the main factor is probably a spin restriction in the charge recombinations. This is absent in the scavenging reaction, which occurs between a radical and a diamagnetic species. Owing to the spin statistics, a reduction of the rate constant by a factor of 4 results when the recombinations cannot lead to formation of an excited triplet state of the product Met or TEA, which seems likely because the triplet energies of these saturated compounds are expected to be quite high.

Electron Decay. As Figure 4 shows, the decay of the electron peak seems to obey a first-order rate law despite the complex kinetics. This deceptively simple behavior also extends to a linear dependence of the apparent rate constant k_{obs} on the starting concentration a_0 of the quinone, suggesting that $e^{\bullet-}_{aq}$ disappears predominantly through scavenging by A with k_{obs}, eq 8. However, this is immediately ruled out by the fact that the signal rise of $A^{\bullet-}$ exhibits a considerably smaller amplitude than does the electron decay (compare Figure 3). Loss of spin polarization by relaxation cannot account for this discrepancy because T_1 is too long to play a significant role on the pertinent time scale. Hence, $e^{\bullet-}_{aq}$ must decay through other channels not leading to $A^{\bullet-}$.

Considering disappearance of $e^{\bullet-}_{aq}$ through self-termination (eq 16) and charge recombination with $D^{\bullet+}$ (eq 17) in addition to scavenging by the starting material A (eq 8), and using the balance equations

$$[A] + [A^{\bullet-}] = a_0 \tag{20}$$

$$[e_{aq}^{\bullet-}] + [A^{\bullet-}] = [D^{\bullet+}] \tag{21}$$

the second of which is not valid in the presence of secondary transformations of $D^{\bullet+}$ but holds approximatively during the early stages of the reaction,[13] we arrive at

$$\frac{d}{dt}[e_{aq}^{\bullet-}] = -k_1 a_0 [e_{aq}^{\bullet-}] - (k_{2a} + k_{self})[e_{aq}^{\bullet-}]^2 + (k_1 - k_{2a})[A^{\bullet-}][e_{aq}^{\bullet-}] \tag{22}$$

The third term on the right-hand side of eq 22 can be combined with the first one because the concentration of radical anions does not change very much; since it contains a difference of similar rate constants and since $[A^{\bullet-}]$ is smaller than a_0 by a factor of about 2, it amounts to a small perturbation only.

The solution of the truncated form of eq 22 is

$$[e_{aq}^{\bullet-}] = [e_{aq}^{\bullet-}]_0 \frac{\exp(-\kappa t)}{1 + r[1 - \exp(-\kappa t)]} \tag{23}$$

with $\kappa = k_1 a_0$ and $r = (k_{2a} + k_{self})[e^{\bullet-}_{aq}]_0/(k_1 a_0)$. For r between 1 and 2, as is suggested by the results of the preceding section, the small deviations of $[e^{\bullet-}_{aq}]$ from a true first-order rate law cannot be resolved by our EPR experiments, especially because the convolution with the acquisition pulse according to eq 26 distorts the function of eq 23 in such a way as to flatten out the steeper decay at early times. Series expansion shows that the initial slope k_{obs} is given by $k_1 a_0 + (k_{2a} + k_{self})[e^{\bullet-}_{aq}]_0$. In the course of the reaction, this reduces asymptotically to $k_1 a_0$, i.e., by the factor r. For optically thin samples, the amount of $e^{\bullet-}_{aq}$ formed must scale with the concentration of the primary light-absorbing component A (compare next section). Hence, $[e^{\bullet-}_{aq}]_0$ is proportional to a_0, which explains the linear dependence of the apparent rate constant k_{obs} on a_0. Under the experimental conditions of Figure 4 (bottom), k_{obs} should lie between $k_1 a_0$ and $[k_1 + 1.4(k_{2a} + k_{self})]a_0$. The slope in the plot of k_{obs} against a_0 (Figure 4, top) is thus compatible with the rate constants obtained from the simulations of the preceding section.

It is obvious from the data that the time dependence of the spin-polarized signal of $e^{\bullet-}_{aq}$ is almost exclusively due to the chemical decay; even at the lowest concentration of A, relaxation plays a very minor role only. By the same token, the line width of the electron peak is predominantly determined by the chemical lifetime of this species. Figure 5 displays the full line width (LW) at half-height of the singlet as a function of the apparent first-order rate constant k_{obs}. For an irreversible reaction (rate constant k) and the line width taken in units of the magnetic field, one has[14]

$$LW = LW_0 + 2k/\gamma_e \tag{24}$$

with the natural line width LW_0, $LW_0 = 2/(\gamma_e T_2)$, and the gyromagnetic ratio of the electron γ_e. Because T_2 and T_1 are approximately equal under our experimental conditions (extreme narrowing limit),[15] the effect of LW_0 is already contained in k_{obs}. Hence, the linear relationship of eq 24 reduces to a direct proportionality between LW and k_{obs}. The constant of proportionality $2/\gamma_e$ is calculated to be 1.14×10^{-11} T s, which agrees very well with the slope of the plot in Figure 5.

The results discussed in this section provide an explanation why the formation of hydrated electrons in PET reactions has

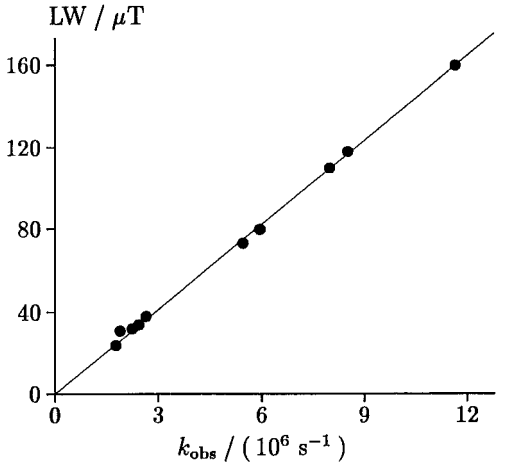

Figure 5. Full width LW at half-maximum of the electron peak as a function of its apparent decay rate k_{obs} in the FT-EPR experiments. Slope of the regression line, 1.37×10^{-11} T s.

not been reported much earlier, given the numerous EPR investigations of photoreactions potentially leading to $e^{\bullet -}_{aq}$, e.g., in quinone/amine systems. With "normal" donor concentrations, however, the disappearance of this intermediate is so rapid as to yield negligible steady-state concentrations; on the other hand, its observation by FT-EPR is rendered impossible by the strong line broadening associated with its decay under these conditions. An additional factor is that—except for scavenging experiments as described in the first section—$e^{\bullet -}_{aq}$ decays to nonspecific products and does not leave a signature in the form of characteristic species that can only be traced back to this intermediate. Therefore, it does not seem unlikely that reinvestigations of other PET systems might reveal the occurrence of $e^{\bullet -}_{aq}$ under conditions of laser flash photolysis.

Intensity Dependence. Figure 6 shows the results of experiments in which the intensity I_{exc} of the exciting light was varied. The geometrical factor remained constant in these measurements, because the optical system was not readjusted between them but only filters were inserted into the optical path. Therefore, a direct comparison of the measured signal intensities (integrals) is meaningful. The displayed initial polarizations of $e^{\bullet -}_{aq}$ and $A^{\bullet -}$ were obtained by the fit procedure described above. They refer to the end of a hypothetical laser flash that is infinitely short on the time scale of the secondary reactions because the kinetic model used for the simulations starts at the radical stage. As discussed, these initial polarizations are proportional to the initial concentrations.

With increasing I_{exc}, the initial concentration of the radical anion grows toward an asymptotic limit. The latter depends on the reactants employed and their concentrations; as already mentioned, it had to be determined by laser flash photolysis with optical detection because of the difficulty of extracting reliable absolute concentrations from the FT-EPR experiments. In contrast to $A^{\bullet -}$, the intensity dependence of the initial concentration of $e^{\bullet -}_{aq}$ shows an upward curvature.

To eliminate the uncertainty of the proportionality factor relating polarizations and concentrations, the ratio of the initial polarizations (i.e., that of the concentrations) of $e^{\bullet -}_{aq}$ and $A^{\bullet -}$ has been plotted at the top of the figure. The increase of this ratio with increasing I_{exc} clearly shows that more than one photon is necessary to generate one electron. Experiments using optical detection reveal that after an induction period this ratio becomes a linear function of I_{exc}, so exactly two photons are consumed in the overall process. The first of these is certainly needed for the PET step; otherwise the electron could not be

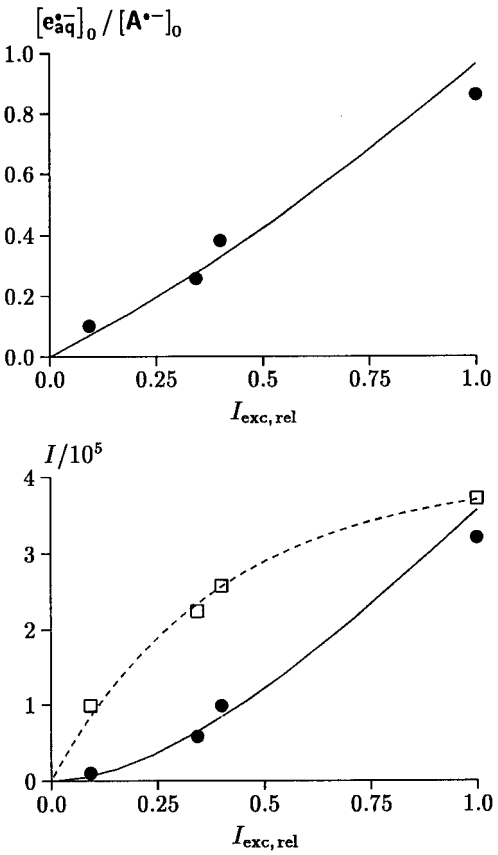

Figure 6. Bottom: dependence of the initial polarizations I of $A^{\bullet -}$ (open squares and broken line) and $e^{\bullet -}_{aq}$ (filled circles and solid line) on the relative intensity $I_{exc,rel}$ of the excitation light. Top: plot of the ratio of these polarizations as a function of the same variable. Experimental parameters: 1.31×10^{-4} M A with 0.1 M Met in 0.1 M aqueous solution of KOH. The fit curves to the data were obtained by numerical solution of the kinetic equations describing the mechanism of Scheme 2.

spin polarized by the triplet mechanism, photoionization of the triplet itself (eq 6) having been ruled out experimentally.

The chemical results presented at the beginning of this work suggest that the species ionized by the second photon is the radical anion of the sensitizer. This is rendered beyond doubt by the two observations that increasing I_{exc} drives the concentration of this intermediate into saturation and that the electron concentration can become much larger than the concentration of the starting quinone (compare Figure 1, bottom). Taken together, these facts can only be reconciled with a mechanism (see Scheme 2) that is cyclic, featuring light-induced regeneration of the starting material, both generation and decay of the intermediate by photoreactions, and formation of the electron by this decay reaction.

The ill-defined geometry of the excited volume, which is due to the noncollimated laser beam and the additional focusing brought about by the cylindrical shape of the EPR tube, preclude an absolute determination of the absorbed light and thus of the quantum yields. Also, the necessary deconvolution and back-extrapolation of the kinetic curves add some uncertainty. For these reasons, a sophisticated evaluation of the EPR-detected light-intensity dependence does not appear to be warranted and we give an approximate treatment.

Owing to the low concentrations and short optical path length, our samples are optically thin with respect to both the quinone and the radical anion. Under these conditions, the Lambert–Beer law can be linearized, and the two excitation steps of the

SCHEME 2

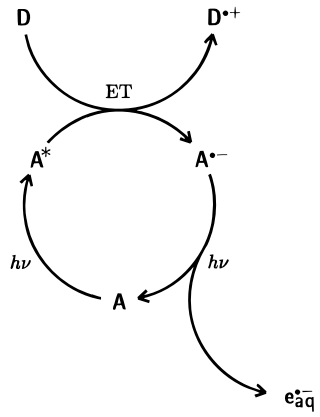

cycle may be described as first-order reactions with rate constants κ_{pet} and κ_{ion} that are both proportional to I_{exc}. The constants of proportionality k_{pet} and k_{ion} comprise the respective extinction coefficient (of A or $A^{\bullet-}$) and the quantum yield of the pertaining process (photoinduced electron transfer of A or photoionization of $A^{\bullet-}$). Owing to the balance equation (eq 20), the steady-state concentration of $A^{\bullet-}$ is $k_{pet}a_0/(k_{pet} + k_{ion})$. In this high-intensity limit, solution of the kinetic equations leads to a linear growth of the electron concentration $[e^{\bullet-}_{aq}]_{lim}$ with I_{exc} according to

$$[e_{aq}^{\bullet-}]_{lim} = \frac{k_{pet}k_{ion}}{k_{pet} + k_{ion}} a_0 I_{exc} \qquad (25)$$

Hence, under these circumstances the ratio $[e^{\bullet-}_{aq}]/[A^{\bullet-}]$ also shows a linear dependence on I_{exc}. Fit curves based on numerical solutions of the differential equations representing the mechanism of Scheme 2 have also been included in the plots of Figure 6 and are seen to reproduce the experimental data quite well. A detailed investigation of the light dependence by laser flash photolysis with optical detection will be published separately.

Conclusions

On the basis of the results obtained in this work we regard it as established that photoinduced electron transfer to A can provide a pathway to $e^{\bullet-}_{aq}$ that is quite efficient. This pathway is not restricted to this particular substrate; in a recent communication[1b] we were able to show by two-flash two-color laser flash photolysis with optical detection that electron formation occurs by the same route in the system 4-carboxybenzophenone quenched by triethylamine. The main difference of the mechanism of Scheme 2 from other known two-photon ionizations with intervening chemical step[16] is that the substrate is regained in the ionization step. As a consequence of this catalytic cycle only the quencher, which is present in high excess anyway, is consumed, but the amount of $e^{\bullet-}_{aq}$ available is not limited by depletion of the substrate. This may well prove to be a decisive advantage and opens up interesting possiblities for technical applications (e.g., initiator systems, decomposition of toxic waste) as well as biological systems, which warrant further investigations.

Experimental Section

The FT-EPR experiments were performed on the spectrometer developed by Dr. D. Beckert at the University of Leipzig. A description of the system can be found in ref 5c. The shortest delay between the laser flash and the sampling pulse was 30 ns. All measurements were carried out at room temperature using $\pi/2$ pulses. Owing to the narrow bandwidth of the microwave pulses, the EPR spectra had to be obtained by combining several measurements at different magnetic fields. A LPSVD software written by Dr. D. Beckert was used to extrapolate the free induction decays to time zero. Further processing of the spectra was done with standard software. Integrals over the EPR signals were determined using line form factors calculated from the simulated EPR spectra as the ratio of the integral to a selected EPR line.[17] This method eliminates baseline distortions, which are frequently encountered in FT-EPR spectra, and is thus much more reliable than other integration routines.

The $\pi/2$ pulses are not δ pulses (i.e., not infinitely short) on the time scale of the kinetics investigated. Sampling a true time-dependent signal I(t) with such a pulse of envelope $\omega(t)$ starting at time T_0 yields[18] an observed signal $I_{obs}(T_0)$

$$I_{obs}(T_0) = \int_0^\infty I(t + T_0)\omega(t) \sin\left(\int_0^t \omega(t')\, dt'\right) dt \qquad (26)$$

This convolution exerts a damping effect on the amplitudes of all time-dependent signals to a degree that is larger the higher their rate of change.

The nominal duration T of the pulse was 24 or 48 ns, depending on the amplifier used. The total rise time τ_r of the pulse, which includes the rise time of the amplifier and that of the B_1 field caused by the high quality factor of the probe, was calculated to be 7 ns. Hence, $\omega(t)$ was described by

$$\omega(t) = \begin{cases} 1 - \exp(-t/\tau_r) & 0 \le t \le T \\ [1 - \exp(-T/\tau_r)] \exp[-(t - T)/\tau_r] & T < t \end{cases} \qquad (27)$$

times a normalization constant to make the integral over the pulse equal to 1. Deconvolution of the experimental intensities was performed by iterative reconvolution of pulse and kinetics and minimizing χ^2. The integral in eq 26 was truncated after $T + 10\tau_r$.

The evaluation software for the fit procedure was written in MATHEMATICA because this high-level language greatly reduces the probability of logical errors in such a complex program without significantly affecting execution time. For the minimization routine, a simplex algorithm[19] was employed because this does not need derivatives and allows easy implementation of parameter constraints and global optimizations. A fractional tolerance of 10^{-9} was used as a termination criterion; however, to ensure convergence, at least one restart of the algorithm from the returned best point was performed.

All parameter constraints were taken into account by modifying the objective function, which returns the sum of the squared deviations between experimental and calculated data points (χ^2). A penalty function was incorporated into this subroutine, taking as its input the allowed interval for each parameter as well as nonnegative scale factors s^2 describing the severity of overstepping the respective limit. Whenever the objective function is called, a test is performed for each variable whether it is confined to the permitted range. If so, a penalty term of unity is assigned to this variable; if not, the amount of overstepping d^2 (i.e., the squared difference between allowed and actual value) is calculated, and the penalty term is increased by the ratio d^2/s^2 taken to a high power (typically, 7). To avoid interference with the minimization routine, the values of the fit parameters are not changed even if they fall outside the allowed interval; however, to eliminate program crashes by out-of-range parameters, χ^2 is calculated with the respective limiting value in this

case. Finally, all penalty terms are multiplied together, and χ^2 times this product is returned to the calling program. The advantages of this procedure over simpler ones, such as setting the objective function to a constant very high value when a limit is overstepped, are that it completely eliminates the possibility of the simplex "hanging" at a border and that it differentiates between violation of the constraints by one or more parameters.

For the EPR experiments, the focused beam (diameter at the entrance slit of the EPR resonator about 3 mm) of an excimer laser (Lambda Physik LPX 105 ESC) operated at 308 ns was directed on a quartz tube (o.d., 3 mm; i.d., 1.4 mm) in the resonator of the spectrometer. The duration of the laser pulse was about 20 ns. To avoid a depletion of the reactants, the repetition rate was kept low (0.5−1 Hz), and a flow system (flow rate about 10 mL/min) was used. From actinometric measurements at the entrance window, the maximum light intensity entering the active volume was estimated to be 15 mJ per flash. The incident light was varied by using metal-grid filters.

For the laser flash photolysis experiments with optical detection an excimer laser (Lambda Physik EMG 101; 308 nm; duration of the excitation pulse ca. 20 ns; about 36 mJ per pulse impinging on the measuring cell) was employed. The dimensions of the excited volume were 4 mm × 2 mm × 2 mm in the directions of the monitoring light, the laser beam, and perpendicular to the preceding two. Again, the repetition rates were kept low and the solutions flowed through the cell. Detection was done in the standard way, except for a photomultiplier (Hamamatsu R 928) with increased sensitivity in the red. The rise time of the detection system was 5 ns, which was essentially limited by the amplifier. Because of the well-defined geometrical arrangement, absolute concentrations of the transients can be reliably determined with this apparatus. It was estimated that the photon fluxes through the samples were comparable in the experiments with optical detection and those with FT-EPR detection.

All chemicals were commercially available in high purity (>99.5%) and used as received. The solvent was ultrapure Millipore MilliQ water (resistance 18.2 MΩ cm^{-1}). In control experiments (photoionization at 308 nm of dilute solutions of the phenolate anion) the half life of $e^{\bullet -}_{aq}$ was found to be about 130 μs under these conditions. Oxygen was carefully removed by bubbling inert gas through the solutions; because the flow systems were made from glass tubing, later diffusion of oxygen into the solutions was avoided.

Acknowledgment. This work was supported by the Volkswagenstiftung. Special gratitude is expressed to Dr. D. Beckert, Universität Leipzig, for generously allowing us to carry out the measurements on his FT-EPR spectrometer and to use his software for preprocessing the spectra.

References and Notes

(1) (a) Zubarev, V.; Goez, M. *Angew. Chem., Int. Ed. Engl.* **1997**, *36*, 2664−2666. (b) Goez, M.; Zubarev, V.; Eckert, G. *J. Am. Chem. Soc.* **1998**, *120*, 5347−5348.

(2) van Willigen, H.; Levstein, P. R.; Ebersole, M. H. *Chem. Rev.* **1993**, *93*, 173−197.

(3) (a) Salikhov, K. M.; Molin, Y. N.; Sagdeev, R. Z.; Buchachenko, A. L. *Spin Polarization and Magnetic Effects in Radical Reactions*; Elsevier: Amsterdam, 1984. (b) Steiner, U. E.; Ulrich, T. *Chem. Rev.* **1989**, *89*, 51−147. (c) Hore, P. J. In *Advanced EPR: Applications in Biology and Biochemistry*; Hoff, A. J., Ed.; Elsevier: Amsterdam, 1989; pp 405−440. (d) McLauchlan, K. A. In *Modern Pulsed and Continuous-Wave Electron Spin Resonance*; Kevan, L., Bowman, M. K., Eds.; Wiley: New York, 1990; pp 285−364.

(4) (a) Goez, M.; Rozwadowski, J.; Marciniak, B. *J. Am. Chem. Soc.* **1996**, *118*, 2882−2891. (b) Goez, M.; Rozwadowski, J.; Marciniak, B. *Angew. Chem., Int. Ed. Engl.* **1998**, *37*, 628−630. (c) Goez, M.; Rozwadowski, J. *J. Phys. Chem. A* **1998**, *102*, 7945−7953.

(5) (a) Beckert, D.; Schneider, G. *Chem. Phys.* **1987**, *116*, 421−428. (b) Beckert, D.; Fessenden, R. W. *J. Phys. Chem.* **1996**, *100*, 1622−1629. (c) Säuberlich, J.; Brede, O.; Beckert, D. *J. Phys. Chem. A* **1997**, *101*, 5659−5665. (d) Säuberlich, J.; Brede, O.; Beckert, D. *Acta Chem. Scand.* **1997**, *51*, 602−609.

(6) Asmus, K.-D.; Göbl, M.; Hiller, K.-O.; Mahling, S.; Mönig, J. *J. Chem. Soc., Perkin Trans. 2* **1985**, 641−646.

(7) Spinks, J. W. T.; Woods, R. J. *An Introduction to Radiation Chemistry*, 2nd ed.; Wiley: New York, 1976.

(8) Verma, C.; Fessenden, R. W. *J. Chem. Phys.* **1976**, *65*, 2139−2155.

(9) Trifunac, A. D.; Nelson, D. J. *J. Am. Chem. Soc.* **1978**, *100*, 5244−5246.

(10) Jeevarajan, A. S.; Fessenden, R. W. *J. Phys. Chem.* **1989**, *93*, 3511−3514.

(11) Hore, P. J.; McLauchlan, K. A. *Mol. Phys.* **1981**, *42*, 1009−1026.

(12) Kausche, T.; Säuberlich, J.; Trobitzsch, E.; Beckert, D.; Dinse, K. P. *Chem. Phys.* **1996**, *208*, 375−390.

(13) In the reactions with Met this assumption might at first glance appear to be questionable almost from the beginning because of the rapid decarboxylation of the radical cations. However, this transformation replaces one electron scavenger ($Met^{\bullet +}$) by another (CO_2) of even higher efficiency.

(14) Ernst, R. R.; Bodenhausen, G.; Wokaun, A. *Principles of Nuclear Magnetic Resonance in One and Two Dimensions*; Oxford University Press: Oxford, 1987.

(15) Carrington, A.; McLachlan, A. *Introduction to Magnetic Resonance*; Harper & Row: New York, 1967.

(16) See, for instance: (a) Nagarajan, V.; Fessenden, R. W. *J. Phys. Chem.* **1985**, *89*, 2330−2335. (b) Redmont, R. W.; Scaiano, J. C.; Johnston, L. J. *J. Am. Chem. Soc.* **1990**, *112*, 398−402. (c) Jent, F.; Paul, H.; Fischer, H. *Chem. Phys. Lett.* **1988**, *146*, 315−319. (d) Faria, J. L.; Steenken, S. *J. Phys. Chem.* **1993**, *97*, 1924−1930. (e) Faria, J. L.; Steenken, S. *J. Chem. Soc., Perkin Trans. 2* **1997**, 1153−1159.

(17) Zeldes, H.; Livingston, R. *J. Magn. Reson.* **1982**, *49*, 84−92.

(18) Goez, M. *Chem. Phys. Lett.* **1990**, *165*, 11−14.

(19) Press, W. H.; Flannery, B. P.; Teukolsky, S. A.; Vetterling, W. T. *Numerical Recipes. The Art of Scientific Computing*; Cambridge University Press: Cambridge, 1986.